Fig. 1: Shifts in the *Plasmodium falciparum* age-antibody curve measure changes in malaria transmission due to intervention in the Garki Project, Nigeria (1970-1976). The intervention included a combination of insecticide spraying and mass drug administration of surfanene-pyrimethamine. Antibody response measured with the IgG indirect fluorescent antibody (IFA) test for *P. falciparum*. **a**, pre-intervention period wet and dry seasons measures (survey rounds 1-2); **b**, active intervention period (survey rounds 3-5, at 20, 50, and 70 weeks following the start of intervention); **c**, post-intervention period (survey rounds 6-8 at 20, 40, and 90 weeks following the end of the intervention). Age-antibody curves, $E(Y_{a,x})$ by age (a) and intervention group (x), were fit using antibody responses in individuals (N=4,774 total measurements, with 153 - 442 measurements per curve) using a nonparametric ensemble machine learning algorithm. Control measurements were combined across survey rounds within each period when plotting the curves to facilitate visual comparison of shifts in transmission between surveys. Age-adjusted geometric means by intervention group, $E(Y_x)$, provide summary differences between curves at each survey round. Error bars show 95% confidence intervals for the age-adjusted geometric means and differences between groups are significant $P \leq 0.01$ (Bonferroni corrected) for all rounds except survey 2. Control villages were not measured in survey 6. **d**, Village-level, age-adjusted geometric mean *P. falciparum* IFA titres, $E(Y_x)$, versus wet season entomological inoculation rate (EIR) in the three study villages with both entomological and serological measurements. Ajura was a control village (no treatment) while Rafine Marke and Nasakar were intervention villages. Labeled points are from the 1971 wet season (pre-intervention) and other points represent wet seasons for 1972-73 (Ajura) or 1972-75 (Rafine Marke and Nasakar). A single data point outside the figure range is not shown (Nasakar 1972, EIR value = 0, $E(Y_x) = 10^{3.0591}$), but was included in the Spearman rank correlation estimate.
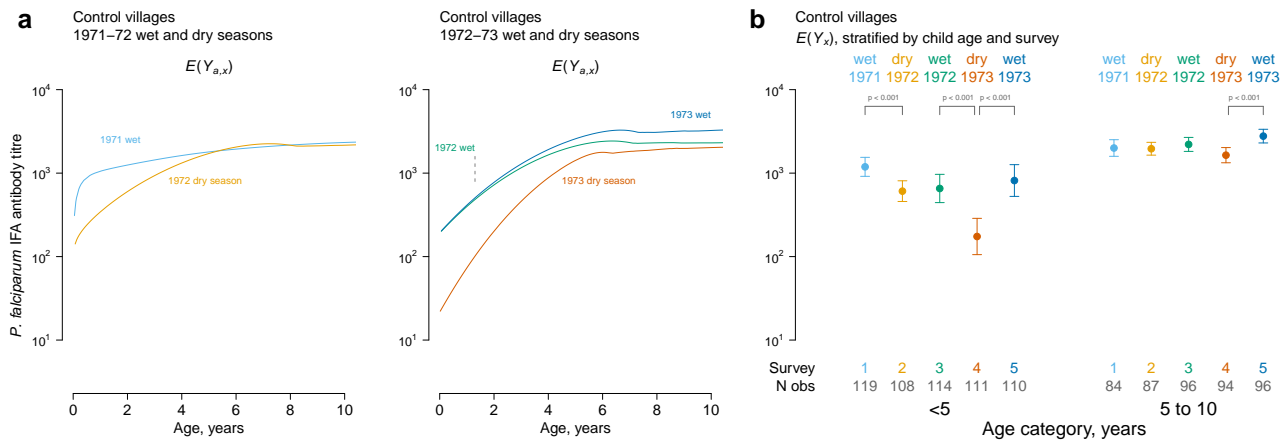
Fig. 2: Higher sensitivity among children <5 y to seasonal changes in *Plasmodium falciparum* transmission as depicted by age-antibody curves estimated within control villages in the Garki Project, Nigeria (1970-1976). Antibody response measured with the IgG indirect fluorescent antibody (IFA) test for *P. falciparum*. **a**, age-antibody curves, $E(Y_{a,x})$ by age (a) and season (x), were fit using antibody responses in individuals as described in Fig 1. **b**, Age-adjusted geometric means by age category and season, $E(Y_x)$, summarize the curves. Error bars show 95% confidence intervals and *P*-values mark significant differences (Bonferroni corrected) between adjacent seasons.
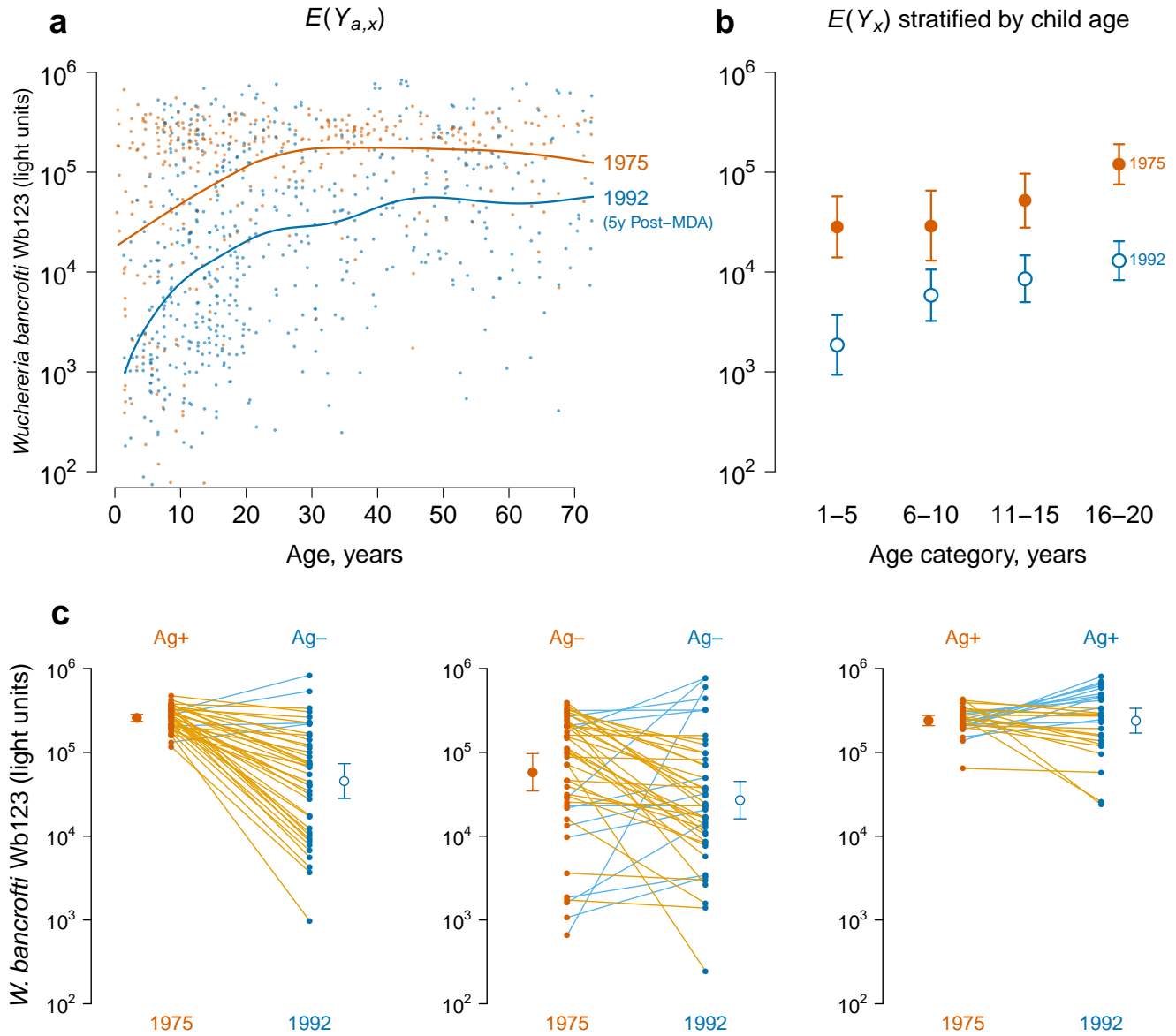
Fig. 3: A shift in the age-antibody curve measures a reduction in transmission of *Wuchereria bancrofti* due to mass drug administration (MDA) on Mauke Island. IgG antibody response to the Wb123 antigen for *W. bancrofti* measured in blood specimens from residents in 1975 (N=362) before MDA and again in 1992 (N=553), five years following a single, island-wide MDA with diethylcarbamazine. Geometric mean antibody levels $E(Y_{a,x})$ by age (a) and survey year (x); individual antibody responses (points) are shown along with summary curves fit with a nonparametric ensemble machine learning algorithm. **b**, Age-adjusted geometric mean antibody response $E(Y_x)$ and 95% confidence intervals before (1975) and five years after (1992) MDA, stratified by 5 year age category (all differences significant at $P \leq 0.01$ after Bonferroni correction). **c**, Wb123 antibody response in 1975 and 1992 stratified by the presence of circulating filarial antigens (Ag) at each measurement in the subsample of 112 individuals who were measured at both time points (two individuals not shown were Ag- in 1975 and Ag+ in 1992), along with age-adjusted geometric means, $E(Y_x)$, and 95% confidence intervals. Differences between means are significant (Bonferroni corrected $P \leq 0.02$) except for the Ag+/Ag+ group. Individual trajectories are colored by the higher of the two measurements: decreases are orange, increases are blue.
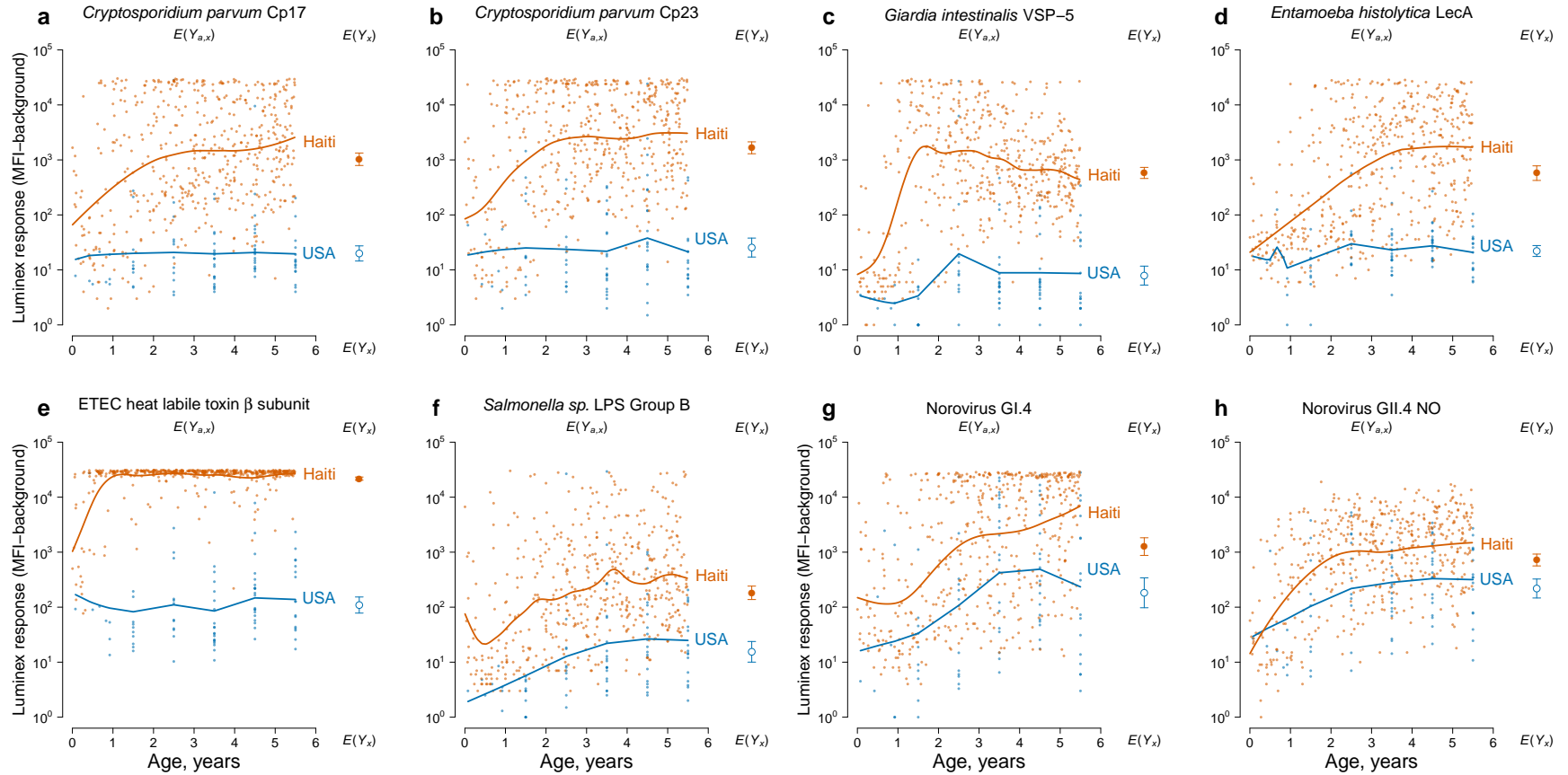
Fig. 4: Differences in enteric pathogen transmission between children in Leogane, Haiti (N=511) and the United States (USA) (N=86) measured by age-antibody curves. Antibody response measured as median fluorescence intensity (MFI) minus background in multiplex bead assays on the Luminex platform. In each panel, individual antibody responses (points) are shown along with age-specific summary curves, $E(Y_{a,x})$, by age (a) and country (x), fit with an ensemble machine learning algorithm. Each panel also includes the geometric mean by country, $E(Y_x)$, with error bars indicating 95% confidence intervals (all differences significant at $P \leq 0.01$ after Bonferroni correction). **a.** *Cryptosporidium parvum* recombinant 17-kDa antigen; **b.** *Cryptosporidium parvum* recombinant 27-kDa antigen; **c.** *Giardia intestinalis* variant-specific surface protein-5 (VSP-5); **d.** *Entamoeba histolytica* lectin adhesion molecule (LecA); **e.** enterotoxigenic *Escherichia coli* (ETEC) heat labile toxin β subunit; **f.** *Salmonella spp.* lipopolysaccharide (LPS) Group B; **g.** Norovirus Group I.4; **h.** Norovirus Group II.4 New Orleans.
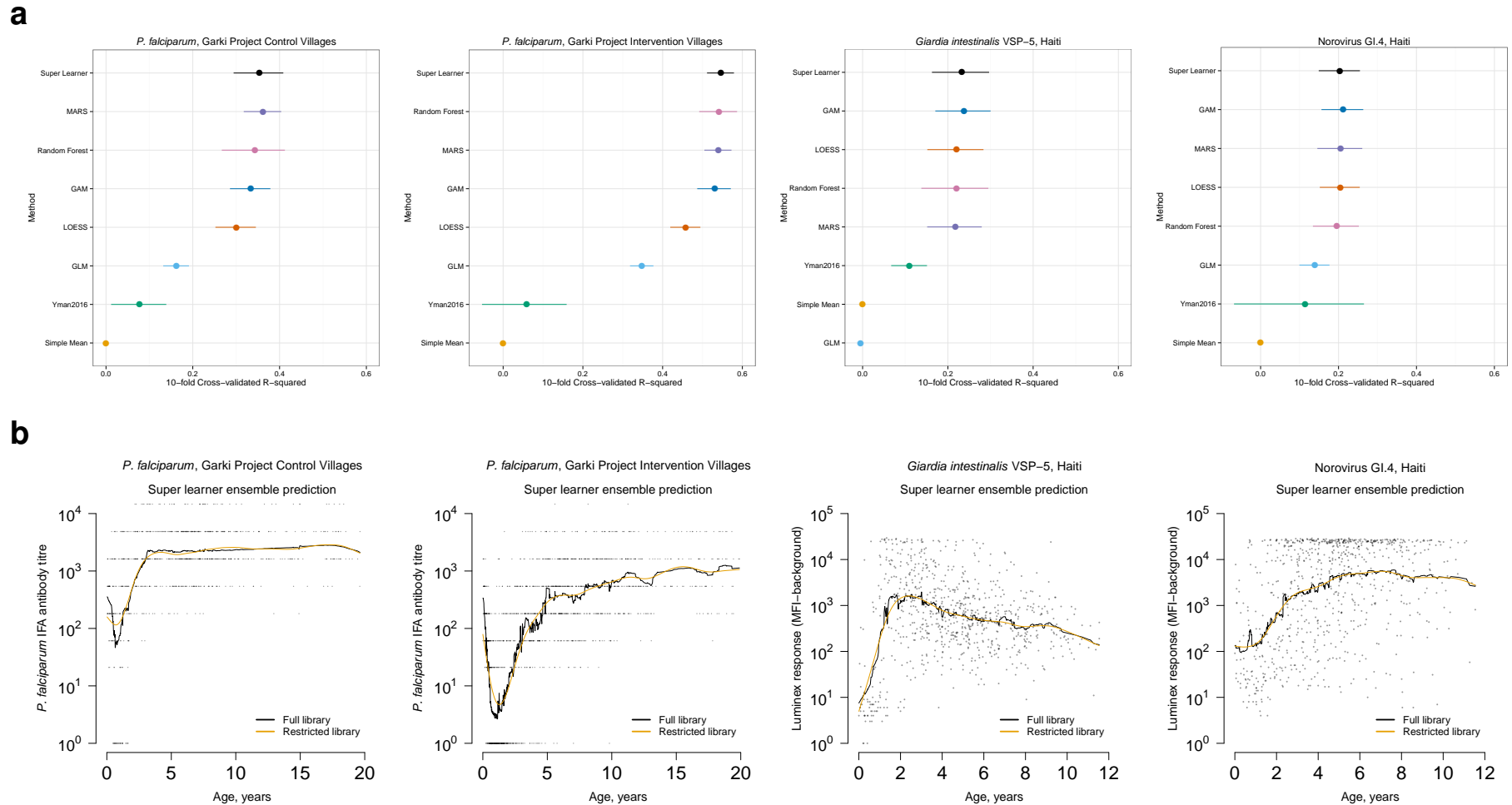
Fig. 5: **a**, Cross-validated estimates of R-squared for the super learner ensemble and its constituent models/algorithms across example populations and pathogens. Cross-validated R-squared is defined as 1− (cross-validated MSE / cross validated var(Y)), and represents the percentage of outcome variability explained beyond estimating the simple mean. Horizontal lines represent twice the standard error of the R-squared estimates measured from 10 random splits of each dataset. In all cases, the algorithms only included age as a feature in antibody level prediction. In the Garki Project, where additional information was available, inclusion of additional covariates (sex, wet vs. dry season, village membership) did not markedly improve R-squared for any algorithm or the ensemble (results available from the authors). **b** Super learner ensemble estimates of age-dependent antibody curves for different populations and pathogens including the full library (all members listed in **a**) as well as a restricted library that excluded two highly adaptive algorithms (Random Forest and MARS). Curves were fit from individual data points included in the plots. *Plasmodium falciparum* IFA antibody titers measured in Garki Project (Nigeria) control and intervention villages during the active intervention period (surveys 3-5). *Giardia intestinalis* variant-specific surface protein-5 (VSP-5) and Norovirus Group I.4 bound antigen measured on the Luminex platform (median fluorescence intensity minus background) in children from Leogane, Haiti. Abbreviations: GAM: generalized additive models with natural splines; GLM: generalized linear model; LOESS: Locally weighted regression; MARS: Multivariate adaptive regression splines; Yman2016: Antibody acquisition model proposed by Yman et al. (*23*).
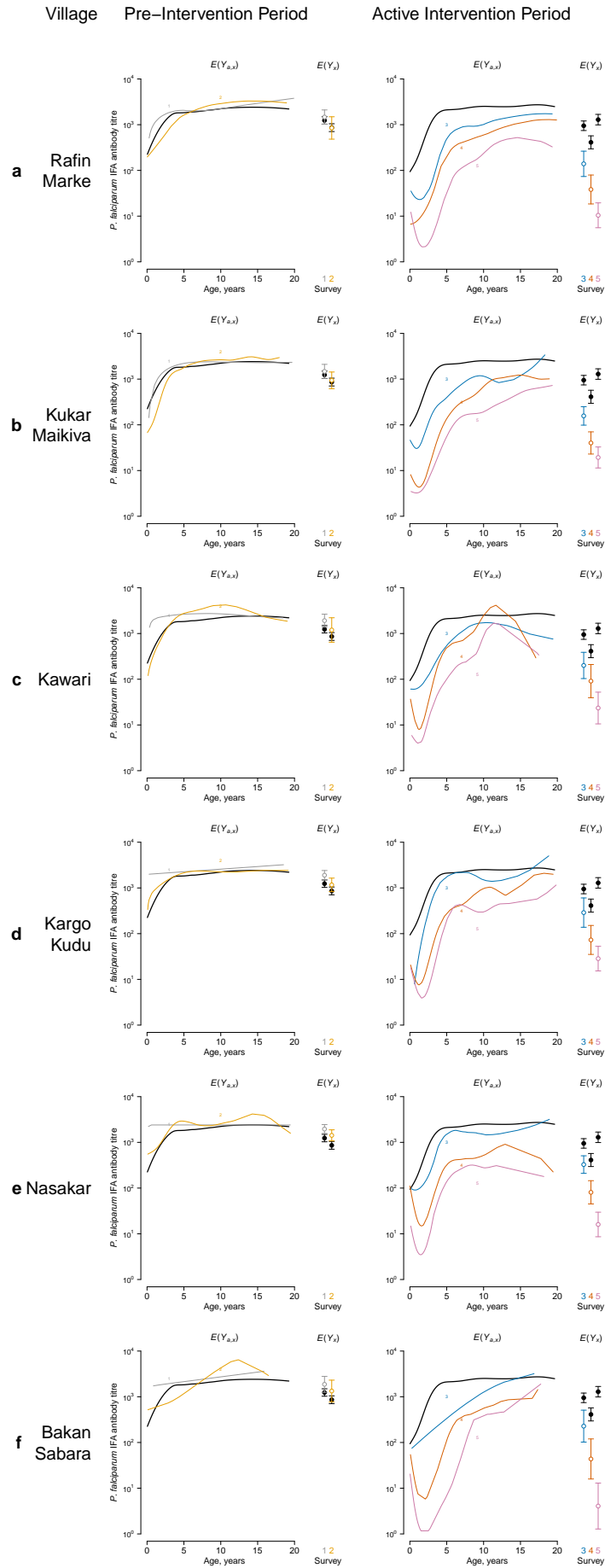
Fig. S1: Caption on the following page.

Fig. S1: *Plasmodium falciparum* age-antibody curves estimated separately for each intervention village (**a-f**) measure reductions in malaria transmission due to intervention in the Garki Project, Nigeria (1970-1976). Antibody response measured with the indirect fluorescent antibody (IFA) test for *P. falciparum*. Panels for each intervention village summarize pre-intervention period wet and dry seasons measures (survey rounds 1-2) and active intervention period (survey rounds 3-5, at 20, 50, and 70 weeks following the start of intervention). Age-antibody curves, $E(Y_{a,x})$ by age (a) and group (x), were estimated non-parametrically from quantitative antibody responses in individuals using an ensemble machine learning algorithm. Age-adjusted geometric means by group, $E(Y_x)$, provide summary differences between curves at each survey round. Error bars show 95% confidence intervals for the age-adjusted geometric means. Each panel includes the same results for the two control villages (black) for comparison. Control measurements were combined across survey rounds within each period when plotting the curves to facilitate visual comparison of shifts in transmission between surveys.
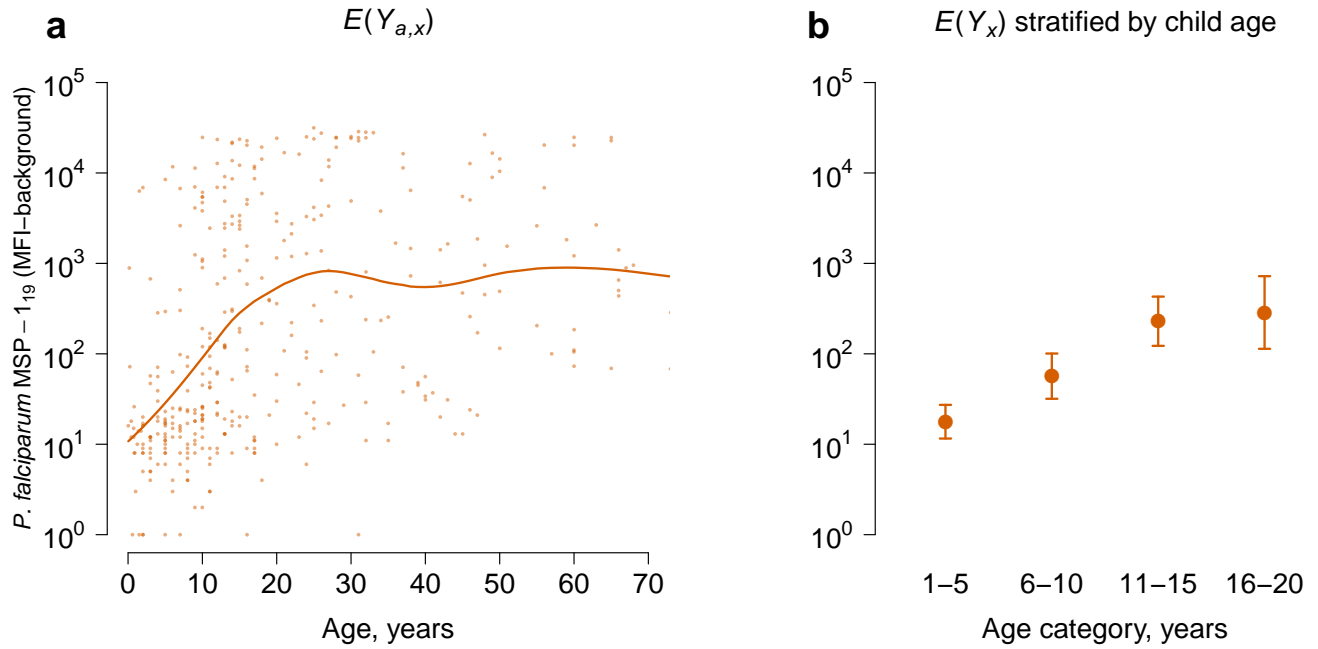
a $E(Y_{a,x})$ **b** $E(Y_x)$ stratified by child age

Fig. S2: Age-antibody curve for IgG antibody response to the *Plasmodium falciparum* merozoite surface protein-1_{19} (MSP-1_{19}) antigen in a 1998 cross-sectional measurement of 383 individuals in the community of Miton, Haiti. A recombinant GST/MSP-1_{19} fusion protein cloned from the *P. falciparum* isolate 3D7 was included in a multiplex bead assay on the Luminex platform. (**a**) Mean antibody levels $E(Y_{a,x})$ by age (a) for ages 0-70 years; individual antibody responses (points) are shown along with a summary curve fit with an ensemble machine learning algorithm. (**b**) Age-adjusted geometric mean antibody response $E(Y_x)$ and 95% confidence intervals stratified by 5 year age category. The number of individuals in each age group was: 1-5 (N=69), 6-10 (N=74), 11-15 (N=68), and 16-20 (N=40). In this example there is no stratification by group (x), but we have left the notation unchanged from other examples to make clear the comparison with other examples in the paper, such as Fig 3.
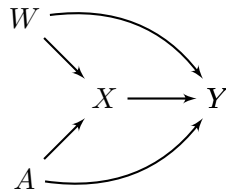
$$
\begin{aligned}
W &= f_W(U_W) \\
A &= f_A(U_A) \\
X &= f_X(A, W, U_X) \\
Y &= f_Y(X, A, W, U_Y)
\end{aligned}
$$

Fig. S3: Structural causal model for a cross-sectional measurement of age (A), antibody level (Y), an exposure of interest (X), and other potentially confounding characteristics (W). For simplicity, the graph omits unmeasured characteristics (U) that, together with each variable's parents, determine what value it takes (e.g., the error term for X is denoted U_X). The equations encode assumptions about time-ordering between variables in the data (e.g., X, A, and W precede Y), but make no assumptions about the functional form of the relationship between them. The equations make no formal assumption about the relationship between errors that generate the data, but under the untestable assumption of no unmeasured common causes of Y and X, (independence of U_Y and U_X), then conditional on A and W mean differences between groups defined by X have a causal interpretation.